



Scenario based Stochastic Multi-Objective Scheduling of Hybrid Heat and Power Resources of a Micro-grid Considering Demand Response Program

Mir Mohammad Mir Mousavi ^a, Gholamreza Salehi^{b,*}, Afshin Mohseni Arasteh ^c, Hassan Feshki Farahani^d, Kamran Lari ^e

^a Department of Energy System Engineering, North Tehran Branch, Islamic Azad University, Tehran, Iran.

^b Department of Mechanical Engineering, Central Tehran Branch, Islamic Azad University, Tehran, Iran

^{c,e} Department of Physical Oceanography, North Tehran Branch, Islamic Azad University, Tehran, Iran

^d Department of Electrical Engineering, Ashtian Branch, Islamic Azad University, Ashtian, Iran.

Corresponding author E-mail address: gh.salehi@iauctb.ac.ir

Abstract: In this paper a stochastic model proposes for optimal microgrid energy management with the aim of minimizing costs and emissions. In this model, uncertainties related to load demand, wind speed and solar irradiation are modeled with a scenario-based stochastic modeling. By using this, the uncertain nature of the proposed problem is converted into some deterministic problems. A Hybrid Microgrid System (HMS) that includes power resources such as wind turbines (WT), photovoltaic panels (PV), energy storage system (ESS), fuel cell (FC), power only unit (PO) and two types of CHP units and heat resources such as heat storage (HS) is set up and programmed in both grid-connected and islanded modes to generate electricity and heat simultaneously. To achieve this goal, network loads will participate in the demand response program (DRP). Since these two goals are not the same, the multi objective particle swarm optimization (MOPSO) algorithm is used to yield the best expected Pareto optimal front. Also, fuzzy-based decision making mechanism is applied to extract the best compromise considering the set of solutions of Pareto optimal front. Due to the high volume of the simulation output, the implemented results are shown only for the 13th scenario as most probable scenario that has a higher probability. Finally, the total cost (\$/day) and total emission (kg/day) for three case studies under each scenario and related expected values are represented.

Keywords: CHP based Micro-grid, demand response program (DRP), Hybrid Heat and Power Resources, MOPSO Algorithm, Stochastic programming.

1. Introduction

The smart micro-grid will face complexities, both in terms of time scale and in terms of technology. Communication requires an extensive connection between the devices using the telecommunications network. In addition, the connection between operating functions such as distribution management systems with advanced load control is also included in the category of communication. In this research, the planning of CHP-based micro-grids is considered. In order to increase its productivity and profit, in addition to generating consumer demand, it also provides thermal energy at the same time. For the study area, the power demand of the loads in the system and the required thermal load for different moments during the scheduling period



Received: 06-06-2024

Revised: 15-07-2024

Accepted: 28-08-2024

can be determined according to the stability in the network and the intelligence of the system. CHP-based micro-grids can be effective and efficient in planning and operating Micro-grids in order to provide loads with power and heat simultaneously.

Ref [1] presents a stochastic model predictive control (MPC) framework to optimally schedule and control the CHP micro-grids with large scale renewable energy resources. A CHP micro-grid consists of CHP, fuel cell units, wind turbines, PV units, battery/ thermal energy storage systems (BESS/ TESS), boilers, electric and thermal loads according to the demand response program. An energy management model based on Mixed-integer linear programming (MILP) with uncertainty variables is proposed. Ref [2] presents the problem of optimal operation and real-time management of the micro-grid based on a fuel cell system, CHP, and battery in order to simultaneously provide energy and heat to the loads by the use of an epsilon-based meta-heuristic method and Fuzzy satisfying method. In Ref [3], the operation of a smart micro-grid has been evaluated from an economic and environmental perspective. In this micro-grid, renewable resources, fuel cell and CHP have been used to simultaneously generate heat and electricity. In this paper, demand response is used as Interruptible loads on the peak demand. Moreover, compromising programming has also been used to solve the problem. In [4], the issue of exploitation of CHP and TES-based micro-grid has been analyzed. In this paper, the TES system is used to control the uncertainty caused by the presence of wind resources, and the differential evolution (DE) algorithm is used to solve the proposed model. In Ref [5], the economically microgrid is planned to provide electric power and heat demand. The combined heat and power-based microgrid needs strategic placement of distributed generators concerning optimal size, location, and type. Also the impact of renewable integration in terms of cost and emission is also investigated. With the focus on the uncertain nature of renewable resources, the issue of predicting wind speed and solar radiation in an MG has been studied in Ref [6]. Ref [7] proposes an optimal scheduling model for regional energy systems to promote clean energy consumption. A multi-objective function that combines the economics and consumption of clean energy is provided. In Ref [8], smart energy management of MG has been examined in terms of cost reduction and pollution. This paper proposes an approach that can solve uncertainty with respect to the fuzzy environment of overall MG operation and uncertainty related to the predicted parameters. The paper [9] proposes an Information Gap Decision Theory (IGDT) - based model for energy hub management, taking into account the demand response (DR). The MG consists of CHP and boiler, energy storage and wind turbine units. The paper [10] aims to optimally design a PV/Wind/Diesel hybrid MG for a small number of houses considering load uncertainty. In Ref [11], the optimal operation of an MG consisting of a fuel cell power plant and the CHP system has been studied using the particle swarm optimization algorithm. In addition, the impact of tariff differences between the purchase and sale of electrical energy at any time of the day has been investigated. A mathematical program for the optimal performance of Micro-CHPs in an MG is provided in Ref [12]. In this context, MG is considered to be connected to the network, which can exchange electricity with the main network. The aim of this model is to reduce final costs if heat demand is provided from the network. The concept and role of DR in MG scheduling are critical, especially with regard to renewable resources. An overview and classification for demand-side management, which analyzes the different types of demand-side management, is presented in Ref [13]. In Ref [14], the DR Quick Distribution Algorithm is developed in the Smart Network. In Ref [15], the effect of DR programs on the voltage stability of electrical systems in the



Received: 06-06-2024

Revised: 15-07-2024

Accepted: 28-08-2024

presence of accidental wind energy production has been studied. The DR Energy Management Plan for the industrial facilities which is proposed in Ref [16] describes the benefits of DER. In Ref [17], a hybrid algorithm, namely JGWO, which combines JAYA and grey wolf optimizer (GWO), has been proposed. The aim is to solve the unit sizing problem of a hybrid system (PV-WT-battery) that can meet consumers' demands at the lowest total annual cost while considering the maximum allowable probability of power supply loss to ensure system reliability. An incentive-based management (IBM) program, with real-time pricing (RTP) and two-sided operation, is presented in [18]. The RTP scheme is proposed for residential load management in [19], also an automatic scheme for the optimal operation of household appliances considering an RTP tariff is presented. The authors in [20] present a framework for economic assessment of storage devices incorporated with photovoltaic (PV) generators considering nine storage technologies. Simultaneous performance of generation and storage units are optimized for two different cases based on time of use (TOU) pricing policy and real-time wholesale of generated power policy. A consumption schedule framework based on game theory is presented in [21] that integrate renewable energy production. The proposed optimization scheme in this paper is based on Mixed-integer programming for scheduling the consumption of residential customers. In [22], it is proposed a two-stage optimization approach with a hybrid demand response program considering a risk index for MG under uncertainty. A multi-objective self-scheduling optimization problem of MG considering the DR program is studied in Ref [23]. This model aims to reduce the final operating cost of the CHP system and reduce the pollution from production units in MG. Besides, in the proposed DR program, there is a load that can be removed at intervals. A model for operating an energy hub-based multiple energy generation micro-grid as combined cooling, heat, and power systems is optimized using the demand response program is developed in [24-25].

As a research gap and scientific contributions of this research, in this research, In addition to renewable sources, two different types of CHP units, electrical and thermal storage sources, and uncertainty in load demand, wind speed, and solar radiation have been taken into account and stochastic modeling has been done with the scenario-based method and is optimized in a multi-objective manner. This paper aims to optimally scheduling of FC/CHP/PV/WT/PO/ESS/HS units to meet micro-grid power and heat demands in both the grid-connected and islanded modes considering uncertainty. The main contributions of the paper can be summarized as follow:

- 1- The multi objective approach of problem formulation is adopted for scheduling of a micro-grid considering cost and emission as two objective functions.
- 2- Optimizing FC/CHP/PV/WT/PO/ESS/HS units using MOPSO approach to minimize objective functions and determine the best solution from Pareto front set by fuzzy decision maker.
- 3- Scenario-based stochastic modeling of uncertainties in three variables for the load demand, wind speed and solar irradiance is implemented.
- 4- The impact of TOU demand response program (DRP) on the micro-grid operation cost and emission cost is analyzed.

The remainder of this paper is organized as follows. In section 2, uncertainty modeling via scenario-based approach is described. The problem formulation and power and heat producers modeling are explained in section 3. The optimization process and the proposed approach also



Received: 06-06-2024

Revised: 15-07-2024

Accepted: 28-08-2024

objective function structure are described in section 4. The cases study and results are presented in section 5. Finally, the conclusions are drawn in section 6.

2. Uncertainty modeling via scenario-based approach

Due to the uncertainty in the load demand of micro-grids and the power generation of renewable energy sources due to wind speed and solar irradiance uncertainties, the design of micro-grids considering the issue of uncertainty has become one of the main challenges for distribution system designers. In this paper, scenario generation method is used to cover the uncertainty of system design parameters. In this method, using Monte Carlo simulation, a number of random states are generated for the system variables based on the probability distribution function of the system variables, and then the probability of occurrence of each state is calculated.

2.1. Scenario generation

Uncertainties are modeled based on their error, which is determined by the probability distribution function (PDF). For example, a typical continuous PDF along with its discretization is shown in Figure (1) for load prediction error [26]. The probability distribution of a random variable is represented by a limited set of scenarios. This method is common in stochastic programming. In this paper, the load demand, output power of PV and WT levels for each scenario was presented as a three-level probability distribution function.

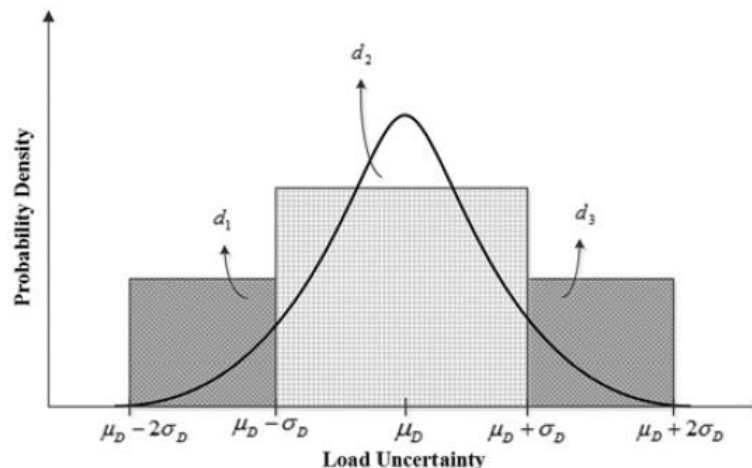


Fig. 1. Typical discretisation of the PDF of the load.

2.2. Scenario reduction

To reduce the computational volume and increase the speed of program execution, scenario reduction using the backward method has been used. This method guarantees the required accuracy of the problem despite reducing the computational volume of the problem and improving the speed of its execution. Scenario reduction is a method to optimally select useful scenarios from a set of generated scenarios, which reduces the execution time of the algorithm and also greatly reduces the computational complexity of the problem. The steps of applying the backward method are as follows [26]:



Received: 06-06-2024

Revised: 15-07-2024

Accepted: 28-08-2024

Consider $\xi_s (s = 1, 2, \dots, N_s)$ as different N_s scenarios, each with a probability of π_s and $DT_{s,s'}$ as distance of scenario pair (s, s') . For using the simultaneous backward method following steps should be applied:

Step1: Consider S as an initial set of scenarios, DS is the scenarios which should be deleted. The initial DS is null. Compute the distances of all scenario pairs: $DT_{s,s'} = DT(\xi_s, \xi_{s'})$, $s, s' =$

$$1, 2, \dots, N_s \text{ as } DT_{s,s'} = \sqrt{\sum_{i=1}^d (v_i^s - v_i^{s'})^2}$$

Step 2: for each scenario k , $DT_{k,r} = \min(DT_{k,s'})$, $s', k \in S$ and $s' \neq k$, I is the scenario index which has the minimum distance with scenario k .

Step 3: Calculate $PD_{k,r} = \pi_k \times DT_{k,r}$, $k \in S$. Select d in which $PD_d = \min(PD_k)$, $k \in S$.

Step 4: $S = S - \{d\}$, $DS = DS - \{d\}$, $\pi_r = \pi_r - \pi_d$

Step 5: Repeat steps 2–4 till the number is mitigated meet our favorite request.

In this work, the proposed stochastic framework considered three uncertain parameters including load demand, solar irradiance, and wind speed. The continuous probability density functions (PDFs) of wind speed, solar irradiance, and loads are used for representing the uncertainties of these parameters; then, the scenario based method is utilized for generating a set of scenarios from combinations of these parameters.

2.3. Modeling of Load Demand

The load demand is presented by normal PDF ($f_d(P_d)$) for uncertainty modeling, which can be expressed using the following equations [27]:

$$f_d(P_d) = \frac{1}{\sigma_d \sqrt{2\pi}} \exp \left[-\frac{(P_d - \mu_d)^2}{2\sigma_d^2} \right] \quad (1)$$

The probabilities and generated load scenarios obtained from (1) can be described as follows:

$$\pi_{d,i} = \int_{P_{d,i}^{min}}^{P_{d,i}^{max}} \frac{1}{\sigma_d \sqrt{2\pi}} \exp \left[-\frac{(P_d - \mu_d)^2}{2\sigma_d^2} \right] dP_d \quad (2)$$

$$P_{d,i} = \frac{1}{\tau_{d,i}} \int_{P_{d,i}^{min}}^{P_{d,i}^{max}} \frac{P_d}{\sigma_d \sqrt{2\pi}} \exp \left[-\frac{(P_d - \mu_d)^2}{2\sigma_d^2} \right] dP_d \quad (3)$$

Three load scenarios are represented in this work. Table (1) provides the probabilities and load scenarios when μ_d and σ_d are 70 and 10.

Table 1. The generated scenarios of the uncertain parameters

Load Scenario	$\pi_{d,i}$	Loading %
1	0.1587	54.7486
2	0.6827	70.0000
3	0.1587	85.2514
Wind Scenario	$\pi_{wind,z}$	Wind speed (m/s)
1	0.7902	7.4518
2	0.1694	13.6153
3	0.0404	17.7289
Irradiance Scenario	$\pi_{solar,m}$	Solar Irradiance (w/m ²)
1	0.1605	416.0627
2	0.4412	609.1166
3	0.3983	790.4621



Received: 06-06-2024

Revised: 15-07-2024

Accepted: 28-08-2024

2.4. Modeling of Wind speed

The uncertainties of wind speed are represented using Weibull PDFs ($f_v(v)$) which can be described as follows [27]:

$$f_v(v) = \left(\frac{k}{c}\right) \left(\frac{v}{c}\right)^{k-1} e^{-(v/c)^k}, \quad 0 \leq v < \infty \quad (4)$$

The wind turbine output power can be provided as follows:

$$P_{WT}(V) = \begin{cases} 0 & 0 \leq v_w \leq v_{wi} \text{ or } v_{wo} \leq v_w \\ P_{wr} \times \frac{v_{wo} - v_{wi}}{v_{wr} - v_{wi}} & v_{ci} \leq v_w \leq v_{wr} \\ P_{wr} & v_{wr} \leq v_w \leq v_{wo} \end{cases} \quad (5)$$

V_{ci} , V_r and V_{co} are the cut-in, rated, and cut-out speeds, respectively. $P_{WT,r}$ is the rated speed of the wind turbine.

The probabilities and generated wind speeds can be presented as follows:

$$\pi_{wind,z} = \int_{v_z^{min}}^{v_z^{max}} \left(\frac{k}{c}\right) \left(\frac{v}{c}\right)^{k-1} e^{-(v/c)^k} dv \quad (6)$$

$$v_z = \frac{1}{\pi_{wind,z}} \int_{v_z^{min}}^{v_z^{max}} \left(\frac{k}{c}\right) \left(\frac{v}{c}\right)^{k-1} e^{-(v/c)^k} dv \quad (7)$$

Three scenarios of wind speed are generated in this work. The wind speed scenarios and their probabilities are listed in Table (1) in the case of selecting c and k to be 10.0434 and 2.5034, respectively.

2.5. Modeling of Solar Irradiance

The solar irradiance using Beta PDF is represented to uncertainty modeling, which can be given as follows [27]:

$$f_G(G) = \begin{cases} \frac{\Gamma(\alpha + \beta)}{\Gamma(\alpha)\Gamma(\beta)} \times G^{\alpha-1} \times (1 - G)^{\beta-1}, & \text{if } 0 \leq G \leq 1, \quad 0 \leq \alpha, \beta \\ 0, & \text{otherwise} \end{cases} \quad (8)$$

$$\beta = (1 - \mu_s) \times \left(\frac{\mu_s \times (1 + \mu_s)}{\sigma_s^2}\right) - 1 \quad (9)$$

$$\alpha = (1 - \mu_s) \times \left(\frac{\mu_s \times \beta}{(1 - \mu_s)}\right) - 1 \quad (10)$$

The output power from the PV system can be described as follows:

$$P_s(G) = \begin{cases} P_{sr} \left(\frac{G^2}{G_{std} \times X_c}\right) & \text{for } 0 < G \leq X_c \\ P_{sr} \left(\frac{G}{G_{std}}\right) & \text{for } G \geq X_c \end{cases} \quad (11)$$

which, G_{std} is set to be 1000W/m², and X_c is a certain irradiance point is set to be 120 W/m². Three scenarios can be obtained by dividing the PDF into three intervals. The portability of solar irradiance for each scenario is given as follows:

$$\pi_{solar,m} = \int_{G_m^{min}}^{G_m^{max}} f_G(G) dG \quad (12)$$

$$G_m = \frac{1}{\pi_{solar,m}} \int_{G_m^{min}}^{G_m^{max}} \left(\frac{\Gamma(\alpha+\beta)}{\Gamma(\alpha)\Gamma(\beta)}\right) \times G^{\alpha-1} \times (1 - G)^{\beta-1} dG \quad (13)$$



Received: 06-06-2024

Revised: 15-07-2024

Accepted: 28-08-2024

The probabilities and generated scenarios of the solar irradiance are provided in Table (1) in the case of selecting α and β to be 6.38 and 3.43, respectively.

2.6. The Combined Load and Generation Model

To model uncertainties of the load demand, wind speed, and irradiance simultaneously, the probabilities of these parameters are multiplied together according to (14) as follows [27]:

$$\pi_S = \pi_{d,i} \times \pi_{wind,k} \times \pi_{solar,m} \quad (14)$$

A total of 27 scenarios can be obtained from (14). Table (2) shows the obtained scenarios and the value of the uncertain parameters and their probabilities.

Table 2. The combined scenarios and their probabilities

Scenario	Loading %	Wind speed (m/s)	Solar Irradiance (w/m ²)	$\pi_{d,i}$	$\pi_{wind,z}$	$\pi_{solar,m}$	π_S
S1	54.7486	7.4518	416.0627	0.1587	0.7902	0.1605	0.0201
S2	54.7486	13.6153	416.0627	0.1587	0.1694	0.1605	0.0043
S3	54.7486	17.7289	416.0627	0.1587	0.0404	0.1605	0.0010
S4	54.7486	7.4518	609.1166	0.1587	0.7902	0.4412	0.0553
S5	54.7486	13.6153	609.1166	0.1587	0.1694	0.4412	0.0119
S6	54.7486	17.7289	609.1166	0.1587	0.0404	0.4412	0.0028
S7	54.7486	7.4518	790.4621	0.1587	0.7902	0.3983	0.0499
S8	54.7486	13.6153	790.4621	0.1587	0.1694	0.3983	0.0107
S9	54.7486	17.7289	790.4621	0.1587	0.0404	0.3983	0.0026
S10	70.0000	7.4518	416.0627	0.6827	0.7902	0.1605	0.0866
S11	70.0000	13.6153	416.0627	0.6827	0.1694	0.1605	0.0186
S12	70.0000	17.7289	416.0627	0.6827	0.0404	0.1605	0.0044
S13	70.0000	7.4518	609.1166	0.6827	0.7902	0.4412	0.2380
S14	70.0000	13.6153	609.1166	0.6827	0.1694	0.4412	0.0510
S15	70.0000	17.7289	609.1166	0.6827	0.0404	0.4412	0.0122
S16	70.0000	7.4518	790.4621	0.6827	0.7902	0.3983	0.2149
S17	70.0000	13.6153	790.4621	0.6827	0.1694	0.3983	0.0461
S18	70.0000	17.7289	790.4621	0.6827	0.0404	0.3983	0.0110
S19	85.2514	7.4518	416.0627	0.1587	0.7902	0.1605	0.0201
S20	85.2514	13.6153	416.0627	0.1587	0.1694	0.1605	0.0043
S21	85.2514	17.7289	416.0627	0.1587	0.0404	0.1605	0.0010
S22	85.2514	7.4518	609.1166	0.1587	0.7902	0.4412	0.0553
S23	85.2514	13.6153	609.1166	0.1587	0.1694	0.4412	0.0119
S24	85.2514	17.7289	609.1166	0.1587	0.0404	0.4412	0.0028
S25	85.2514	7.4518	790.4621	0.1587	0.7902	0.3983	0.0499
S26	85.2514	13.6153	790.4621	0.1587	0.1694	0.3983	0.0107
S27	85.2514	17.7289	790.4621	0.1587	0.0404	0.3983	0.0026

3. Problem formulation

Micro-grids can be used to provide energy efficient, low cost and clean. Using electricity and heat-based micro-grids increases system efficiency and reduces operating costs due to the use of heat wasted in the power generation process to meet heat demand. Considering the environmental issues arising from the use of fossil fuels, the minimization of emissions that is in conflict with economic issues should be considered. In this work, minimizing pollution emissions while maximizing profits makes it a multi-objective problem. Multiple power and heat generation units and storage systems such as CHP, FC, ES units, power and heat only



Received: 06-06-2024

Revised: 15-07-2024

Accepted: 28-08-2024

units, and heat storage in the micro-grid are considered. The structure of two types of CHP-based micro-grid system is shown in Figure (2) [28]. The main purpose of this work is to optimally dispatch power and heat in the micro-grid by maximizing total profit and minimizing emissions, which are conflicting goals. In this way, a multi-objective optimization problem is achieved when connected to the network and islanded from the network. In the grid-connected state, it is assumed that due to the generation of electricity and micro-grid heat, energy is exchanged with the main grid.

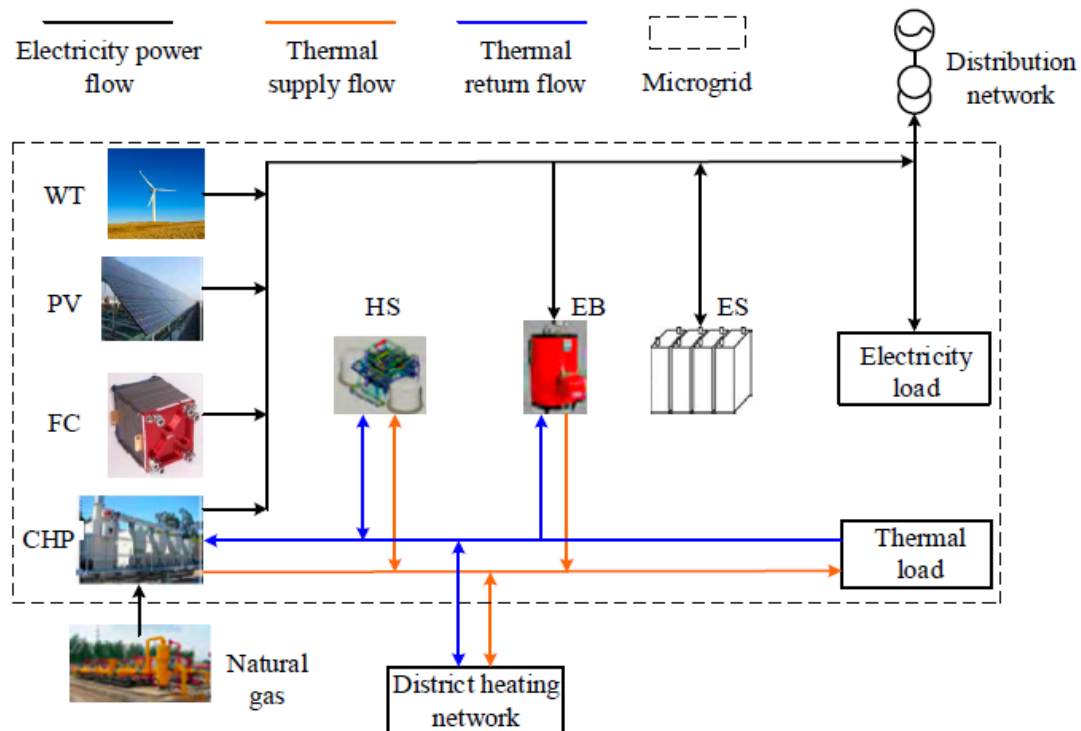


Fig. 2. Structure of CHP-based micro-grid system

3.1. Demand Response Program (DRP)

By implementing time of use (TOU) DR programs, the load can be shifted from more expensive time periods to cheaper time periods, which, according to [29], can delay investment in capacity building and costly energy supply.

TOU-DR program can be formulated by equation (15).

$$P_h^{DR} = P_h^D + ldr_h \quad (15)$$

where, ldr_h , is the amount of shifted load from another level to h-th hour load level. ldr_h , can be calculated by using equation (16).

$$ldr_h = DR_h \times P_h^D \quad (16)$$

where, DR_h is the participation factor of the load in DR program at h-th load level and P_h^D is the initial electric load demand at h-th load level in MWh.

The total amount of shifted load over a daily period is assumed to be equal to zero. This is expressed in equation (17). At each time period, DR_h is limited by equation (18).

$$\sum_{h=1}^{24} ldr_h = 0 \quad (17)$$



Received: 06-06-2024

Revised: 15-07-2024

Accepted: 28-08-2024

$$DR_h^{min} \leq DR_h \leq DR_h^{max} \quad (18)$$

3.2. Fuel Cell unit

The fuel cell is considered as a production unit, which can generate electricity from natural gas and methanol hydrogen-containing fuel. The cost of an FC unit includes the cost of fuel and the efficiency of the fuel to generate electricity expressed as equation (19) [30]:

$$C_{FC} = \sum_{t=1}^T (\beta_{natural} \sum_{i=1}^{N_{FC}} \frac{P_{FC,it}}{\eta_{FC,ei}} + \frac{H_{FC,it}}{\eta_{FC,hi}}) \quad (19)$$

where C_{FC} is the fuel-cell generation cost; $\beta_{natural}$ is the natural gas cost in \$/Kg; $P_{FC,it}$ and $H_{FC,it}$ are the fuel cell electricity and heat generation of the i th unit at time t respectively; $\eta_{FC,ei}$ and $\eta_{FC,hi}$ are the fuel cell electricity and heat efficiency of i th unit respectively; N_{FC} is the number of fuel-cell plants.

3.3. CHP unit's model

Two types of CHP units in micro-grid have been included in this paper and the feasible operating regions (FOR) for each type are shown as Figure (3). CHP's electrical and thermal production power must be located in the enclosed area formed by points A, B, C, D, E and F. If you are interested, refer to reference [31].

Total operation cost of a CHP related to both heat and electricity is modeled by equation (20).

$$C(P_h^{CHP}, H_h^{CHP}) = a \times (P_h^{CHP})^2 + b \times P_h^{CHP} + c + d \times (H_h^{CHP})^2 + e \times H_h^{CHP} + f \times H_h^{CHP} \times P_h^{CHP} \quad (20)$$

where $a, b, c, d, e,$ and f are cost function coefficients of CHP units, P_h^{CHP} and H_h^{CHP} are the power and heat generated by the CHP, respectively.

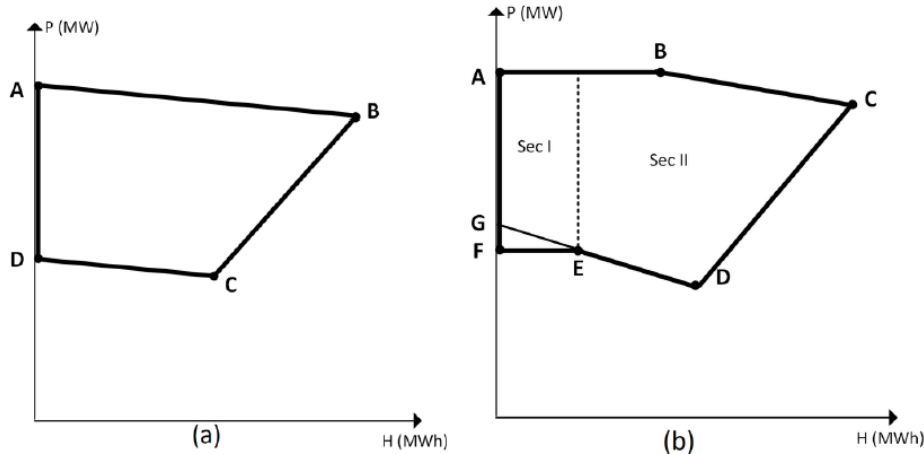


Fig. 3. Feasible region for CHP units (a) Type 1 (b) Type 2

3.4. Power-only and Heat-only unit

Equations (21) and (22) describe operation constraint of power only and heat-only units, respectively.

$$P_h^{PO-min} \times V_h^{PO} \leq P_h^{PO} \leq P_h^{PO-max} \times V_h^{PO} \quad (21)$$

$$H_h^{b-min} \times V_h^b \leq H_h^b \leq H_h^{b-max} \times V_h^b \quad (22)$$

where P_h^{PO} is generated power from power-only unit at time h in MW, P_h^{PO-min} and P_h^{PO-max} are minimum and maximum power limits of power-only unit, H_h^b is generated heat from boiler



Received: 06-06-2024

Revised: 15-07-2024

Accepted: 28-08-2024

unit at time h (MWth), H_h^{b-min} and H_h^{b-max} are minimum and maximum heat limits of boiler unit.

Cost functions of power-only and heat-only units are described by equations (23) and (24).

$$C(P_h^{PO}) = \lambda_{PO} \times P_h^{PO} \quad (23)$$

$$C(H_h^b) = \lambda_b \times H_h^b \quad (24)$$

where $C(P_h^{PO})$ is cost function of power-only unit at time λ_{PO} is the power price of a power-only unit in hour h (\$/MW h), $C(H_h^b)$ is cost function of boiler unit at time h , and λ_b is the price of power of boiler unit in the h -th hour (\$/MWth h).

2.5. Electrical Energy Storage Model

The charge/discharge modes of electrical energy storage (ESS) are modeled as follows:

$$SOC(t) = SOC(t-1) + (P^{ch})\eta_{ch}^{ST} - \frac{P^{dch}(t)}{\eta_{Dch}^{ST}} \quad (25)$$

$$SOC(t_0) = SOC(t_T) \quad (26)$$

$$E_{min}^{st} \leq SOC(t) \leq E_{max}^{st} \quad (27)$$

$$P^{dch}(t) \leq E_{max}^{Dch} \cdot \zeta_{dch} \quad (28)$$

$$P^{ch}(t) \leq E_{max}^{st} \cdot \zeta_{ch} \quad (29)$$

$$\zeta_{ch} + \zeta_{dch} \leq 1 \quad (30)$$

Where $SOC(t)$ is the state of charge at time t , η_{ch}^{ST} and η_{Dch}^{ST} are the charging and discharging efficiencies respectively; P^{ch} and P^{dch} are the charged and discharged power, respectively; the parameters E_{min}^{st} and E_{max}^{st} are the minimum and maximum capacities of the ESS; and ζ_{ch} and ζ_{dch} are binary variables to show the charge/discharge state of battery. It can be seen in Equation (25) that the SOC in each hour is obtained by considering the charging and discharging amounts of the ESS in that hour. Based on Equation (26), the SOC at the beginning and the end must be equal. The SOC is limited by its bound in Equation (27). The amount of charging/discharging is limited to the maximum capacity of the ESS in Equations (28) and (29). According to Equation (30), the charging and discharging modes cannot occur simultaneously.

3.5. Heat Storage (HS)

The total generated heat is calculated by equation (31).

$$H_h = \sum_{i=1}^{N_{CHP}} H_{i,h}^{CHP} + H_h^b + H_h^{FC} \quad (31)$$

By using $\beta_{gain}/\beta_{loss}$ which is heat generation loss/excess of the CHP unit during startup/shutdown period, heat losses during shutdown and startup periods can be modeled by equation (32). The available heat capacity at each time interval in the heat storage, B_h , is expressed by equation (33).

$$H_h = \bar{H}_h - \beta_{loss} SU_h^f + \beta_{gain} \cdot SD_h^i; \quad i \in FC, CHP, b \quad (32)$$

$$B_h = (1 - \eta) \times B_{h-1} + H_h - H_h^{load} \quad (33)$$

where, η is heat loss rate for the heat storage.

By using equation (34), the maximum available capacity of heat storage can be limited.

$$B_{min} \leq B_h \leq B_{max} \quad (34)$$

where $B_{min}=B_{max}$ is minimum/maximum heat storage capacity in MW.



Received: 06-06-2024

Revised: 15-07-2024

Accepted: 28-08-2024

Equations (35) and (36) are applied to model the ramping up/down rates for the heat storage system.

$$B_{h-1} - B_h \leq B_{max}^{charge} \quad (35)$$

$$B_{h-1} - B_h \leq B_{max}^{discharge} \quad (36)$$

where $B_{max}^{charge} / B_{max}^{discharge}$ is the maximum charge/discharge rate of the storage MWth.

3.6. Start up and shutdown status

The startup and shutdown statuses of each unit can be modeled by equations (37) and (38).

$$SU_h^i = V_h^i \times (1 - V_{h-1}^i) \quad i \in FC, CHP, PO, b \quad (37)$$

$$SD_h^i = (1 - V_h^i) \times V_{h-1}^i \quad i \in FC, CHP, PO, b \quad (38)$$

3.7. Power balance

With considering DR program, generated power should meet the load demand at each hour using equation (39).

$$P_h^{G,byu} - P_h^{G,sell} + \sum_{i=1}^{N_{CHP}} P_{i,h}^{CHP} + P_h^{FC} + P_h^{PO} + P_h^{disc} - P_h^C - P_h^{DR} = 0; \forall h \quad (39)$$

where, P_h^{DR} is the electric load demand after applying DR program at h- th load level.

4. Optimization method

4.1. MOPSO algorithm

In this paper, the optimization problem is a continuous problem and also due to the capabilities of the PSO algorithm in terms of high accuracy and higher convergence rate than other algorithms, the multi-objective version of this algorithm is used to solve the problem. Multi-objective problems composed of multiple inconsistent objective functions, and equality and inequality constraints terms, like the one written below, which should be optimized [32].

$$\text{Min } F(\vec{X}) = [f_1(\vec{X}), f_2(\vec{X}), \dots, f_N(\vec{X})]^T$$

Subject to:

$$g_i(\vec{X}) < 0 \quad i = 1, 2, \dots, N_{ueq} \quad (40)$$

$$g_i(\vec{X}) = 0 \quad i = 1, 2, \dots, N_{eq}$$

The space within which the objective function is defined is called objective space. In multi-objective optimization, every two definitions can be described and have two different states with respect to each other as expressed in equation (41):

- One solution can dominate the other one
- No solution can dominate the other solution,

$$\forall j \in \{1, 2, \dots, n\}, f_j(\vec{X}_1) \leq f_j(\vec{X}_2) \quad (41)$$

$$\exists k \in \{1, 2, \dots, n\}, f_k(\vec{X}_1) < f_k(\vec{X}_2)$$

By applying the Pareto optimal concepts using fundamental principles in Particle Swarm Optimization (PSO) algorithm, this algorithm is accustomed to solve multi-objective problems called Multi-Objective Swarm Particle Optimization (MOPSO) [33]. In MOPSO algorithm, a repository is employed to save lots of solutions. Repository means an external memory on which the dominated solutions will be saved. This algorithm first starts to figure employing a series of random particles. All the population particles are compared with one another during



Received: 06-06-2024

Revised: 15-07-2024

Accepted: 28-08-2024

a repeated procedure and position of the dominated particles is saved on the repository. All steps and flowchart of MOPSO algorithm implementation are presented in detail in reference [32].

4.2. Objective function

In this study, two objective functions are considered in a multi-objective function. It is worth mentioning that in case of considering the uncertainties in parameters; a set of scenarios will be generated. Thus, these scenarios should be considered for the efficient solving of problem, and expected values are used to evaluate the effect of uncertainty in each case study as depicted in the following equations. In this work, the considered objective function is a multi-objective function comprising two objective functions which can be presented as follows:

4.2.1. Minimization of Expected Total Cost (TCost)

The total cost objective function, OF1, is defined as terms such as revenue from the selling electricity to the grid, the cost of electricity purchased from the upstream grid and the cost of producing heat, and the cost of energy storage system degradation. Equation (42) describes the first objective function.

$$\begin{aligned}
 OF_1 = TCost_S = & \sum_{h=1}^{24} \lambda_h \times P_h^{G,buy} \\
 & + \sum_{i=1}^{N_{CHP}} C(P_{i,h}^{CHP}, +H_{i,h}^{CHP}) + C_{FC} + C(P_h^{PO}) + C(H_h^b) \\
 & + \sum_{j \in \{FC, CHP, PO, b\}} (C_{j,SU} \cdot SU_h^j + C_{j,SD} \cdot SD_h^j) \\
 & + C_k^{deg} \left(\sum_{k=1}^{N_k} \frac{P_{k,h}^{disc}}{\eta_k^{disc}} + \eta_k^c \times P_{k,h}^C \right) - \lambda_h \times P_h^{G,sell}
 \end{aligned} \tag{42}$$

$$ETCost = \sum_{S=1}^{N_S} \pi_S \times TCost_S \tag{43}$$

where λ_h is the price of power at time h in (\$/MWh), $P_h^{G,sell}$ and $P_h^{G,buy}$ are the amount of electricity sold and purchased power to or from the network at time h (MWh), $C(P_{i,h}^{CHP}, +H_{i,h}^{CHP})$ are the CHP, FC, PO, HO units cost function, respectively, $C_{j,SU}$ and $C_{j,SD}$ are startup and shutdown costs of generation facility in dollar, respectively, SU_h^j and SD_h^j are binary variables of start-up or shut down status for the units at time h, C_k^{deg} is cost for battery degradation in \$/kWh, $P_{k,h}^C$ and $P_{k,h}^{disc}$ are charged and discharged power of the battery in kW, respectively.

4.2.1. Minimization of Expected Total Emission (ETEmission)

Pollution emissions of MG, OF2, are considered as the second objective function which is described by equation (44).



Received: 06-06-2024

Revised: 15-07-2024

Accepted: 28-08-2024

$$OF_2 = ETEmission_s = \sum_{h=1}^{N_h} (E_h^{CHP} + E_h^{FC} + E_h^{PO} + E_h^G) \quad (44)$$

$$E_h^{CHP} = \sum_{i=1}^{N_{CHP}} NOx_{i,h} + SO2_{i,h} + CO2_{i,h} = (k_1^{CHP} + k_2^{CHP} + k_3^{CHP}) \times P_{i,h}^{CHP}$$

$$E_h^G = NOx_h^G + SO2_h^G + CO2_h^G = (k_1^G + k_2^G + k_3^G) \times P_h^G E_h^{PO}$$

$$= NOx_h^{PO} + SO2_h^{PO} + CO_h^{PO} = (k_1^{PO} + k_2^{PO} + k_3^{PO}) \times P_h^{PO} E_h^{FC}$$

$$= NOx_h^{FC} + SO2_h^{FC} + CO_h^{FC} = (k_1^{FC} + k_2^{FC} + k_3^{FC}) \times P_{i,h}^{FC}$$

$$ETEmission = \sum_{S=1}^{N_s} \pi_S \times ETEmission_S \quad (45)$$

where E_h^{CHP} , E_h^{FC} , E_h^{PO} , and E_h^G are emission values of each unit in MG (kg/day).

3.3. Fuzzy decision making method

After obtaining the Pareto optimal solution front, planners might have to choose the simplest compromising solution from among the set of optimal solutions. The fuzzy min-max method assigns a fuzzy membership function to every solution within the Pareto front which is within the interval [0, 1]. Equation (46) is employed to urge fuzzy membership functions for the i-th objective function [33].

$$OF_{k,p,u} = \begin{cases} 1 & OF_k \leq OF_k^{min} \\ \frac{f_i^{max} - f_i^k}{f_i^{max} - f_i^{min}} & OF_k^{min} < OF_k < OF_k^{max} \\ 0 & OF_k \geq OF_k^{max} \end{cases} \quad (46)$$

In order to obtain the best final solution, the fuzzy decision making method is implemented. First at all, the minimum value of OF1 and OF2 is obtained, and then the solution with the maximum value of min (OF1, OF2) as the best final solution is being selected.

5. Simulation results

5.1. Input data

The numerical values of emission, data of the fuel cell unit, data of the energy storage device and heat storage, the startup and shutdown costs of units and cost function coefficients of CHP units all are presented in [31]. The FOR data of CHP units are also listed in [31]. Maximum DR is assumed to be 30%. The pollution coefficients of these power generation units are considered zero and the cost of selling electricity for photovoltaic panels and wind turbines are 2.584 €/ct/kwh and 1.073 €/ct/kwh, respectively [33]. Also the maximum projected capacity for determining the capacity of solar power plants and wind turbines is 1.5 MW and 1.2 MW, respectively. The base heat and electric demand of MG are shown in Figure (4). In addition, electric power and heat price are shown in Figure (5).



Received: 06-06-2024

Revised: 15-07-2024

Accepted: 28-08-2024

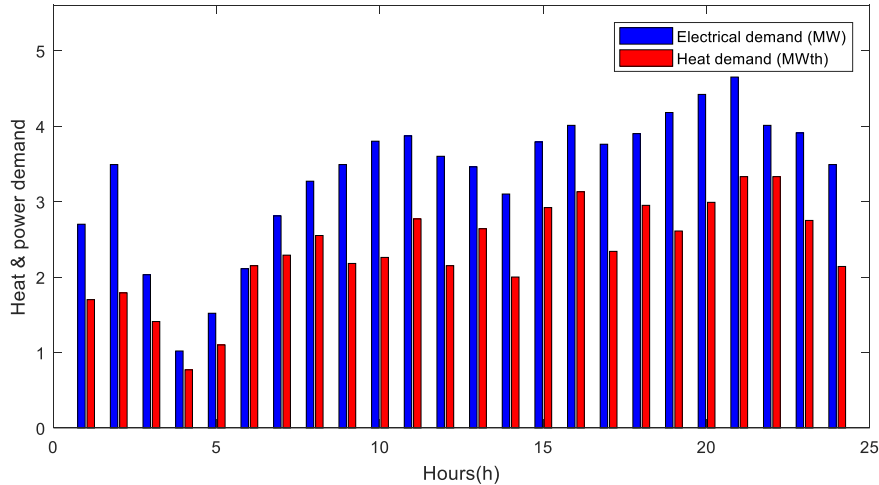


Fig. 4. Electric power and heat demand

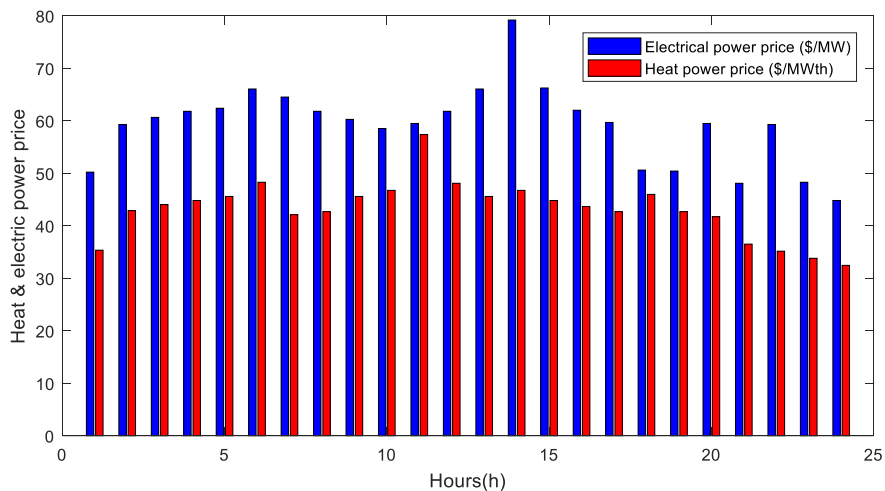


Fig. 5. Electric power and heat price

5.2. Test cases

In this paper, three case studies have been taken into account:

Case A: CHP-FC-PV-WT-ESS based MG scheduling in islanded mode;

Case B: CHP-FC-PV-WT-ESS based MG scheduling in grid-connected mode;

Case C: Impact of TOU-DR program implementing on case B.

In Cases B and C, the MG is able to exchange (sell or purchase) power with the upstream network, according to the market prices as shown in Figure (5).

To solve the optimization problem, at first step MG operator uses MOPSO optimize MG operation with expected scenario. This was simulated by considering the hourly average values of load, wind speed, and solar irradiance. Here, it is assumed that the MG operator must buy all the power produced by the PV/WT at each time of the day. In the second step, risk costs arising from uncertainty are minimized by the MG operator. The 1000 scenarios were generated by considering the uncertainty in the MG via Monte Carlo simulations. Subsequently, 3 scenarios were selected via backward reduction method to each uncertain variable of load, wind speed, and solar irradiance. From the 27 (3*3*3) generated scenarios,



Received: 06-06-2024

Revised: 15-07-2024

Accepted: 28-08-2024

expected total cost and expected emission cost were determined. Only the results of the Pareto solution front related to scenario 13 are presented as the scenario with the highest probability, and the results of other scenarios after selection by the fuzzy decision-making method and the selected best compromise solution are shown in Table (6) to calculate the expected total cost and expected total emissions are used.

Case A: In this case, the islanded mode is taken into account for MG. Table (3) provides the Pareto optimal solutions for scheduling of MG without consideration of DRP for Case A and scenario S13. The maximum weakest membership function of 0.6316 is related to Solution #13. Considering the min-max fuzzy satisfying method, solution #13 is opted as the best compromise solution. According to Table (3), the cost of MG energy production is equal to \$4403.956. Moreover, the emission is obtained as 60984.88 kg/day. The minimum value of operation cost of MG is obtained as \$4227.101, which is related to solution #1 where the aim is to minimize the total cost of MG. Also, the minimum amount of emission provided is equal to 58962.319 kg/day, which is obtained in solution #20 where the minimization of emission is aimed.

Table 3. Pareto optimal solutions for short-term scheduling of micro-grid without DRP (Case-A) for scenario s13 as a highest probability

#	OF1 (\$/day)	OF2 (kg/day)	OF _{1,p.u.}	OF _{2,p.u.}	Min (OF _{1,p.u.} , OF _{2,p.u.})
1	4227.101	64452.02	1.0000	0.0000	0.0000
2	4235.8676	64163.666	0.9835	0.0525	0.0525
3	4244.1936	63874.724	0.9679	0.1052	0.1052
4	4252.5523	63585.54	0.9521	0.1578	0.1578
5	4261.7752	63296.797	0.9348	0.2104	0.2104
6	4276.3422	63007.939	0.9074	0.2631	0.2631
7	4291.9812	62718.826	0.8780	0.3157	0.3157
8	4307.2303	62430.055	0.8493	0.3683	0.3683
9	4322.8506	62141.996	0.8199	0.4208	0.4208
10	4338.6199	61851.76	0.7903	0.4737	0.4737
11	4355.4114	61562.876	0.7587	0.5263	0.5263
12	4384.4309	61273.689	0.7041	0.5790	0.5790
13	4403.956	60984.88	0.6674	0.6316	0.6316
14	4442.949	60695.647	0.5941	0.6843	0.5941
15	4472.1021	60407.017	0.5392	0.7368	0.5392
16	4506.2618	60117.995	0.4750	0.7895	0.4750
17	4569.3486	59829.367	0.3564	0.8421	0.3564
18	4679.5498	59540.568	0.1491	0.8947	0.1491
19	4719.3148	59251.478	0.0743	0.9473	0.0743
20	4758.8403	58962.319	0.0000	1.0000	0.0000

Figure (6) shows the produced power of case A for PV, WT, fuel cell, CHP1, and CHP2 also power-only units for 24 hours. As output of the optimization program, the production capacity of solar cells and wind turbines is 0.59 MW and 0.23 MW, respectively. The production curve of solar cell and wind turbine is shown in this figure for 24 hours. The supplied heat of Case A in the studied time horizon is illustrated in Figure (7). According to this Figure, the heat generation of CHP1 is more than those of other production units. CHP2 has less heat generation than CHP1, since its heat cost is higher than that of CHP1. The boiler and fuel cell units have produced heat in their capacity limits. As it is obvious in figures (6) and (7), considering the



Received: 06-06-2024

Revised: 15-07-2024

Accepted: 28-08-2024

time interval at which the fuel cell has not participated in power and heat generation, the remained capacity of the fuel cell is stored as hydrogen in the hydrogen tank at this time interval.

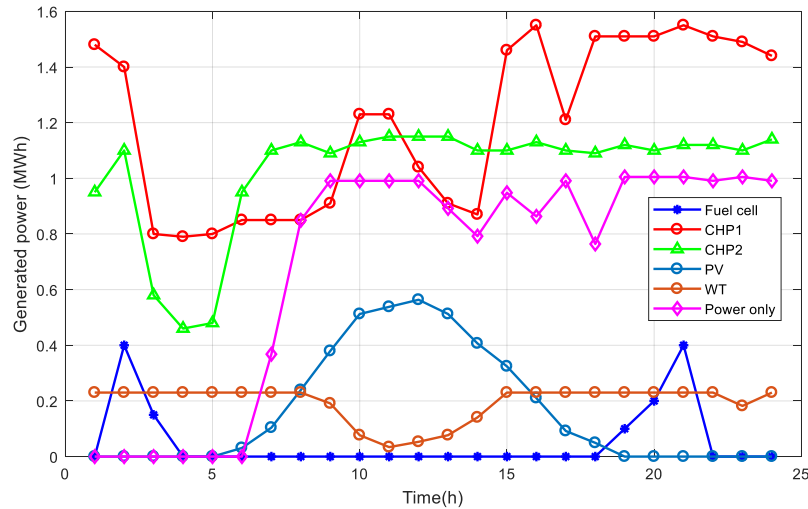


Fig. 6. Generated power of the case A

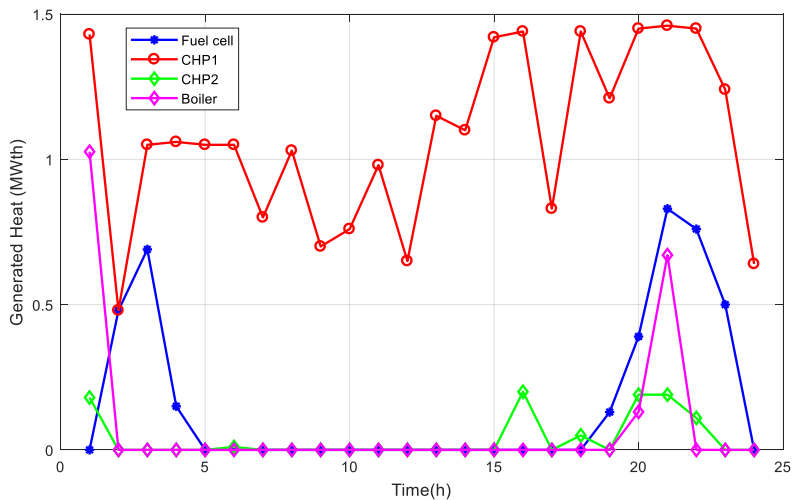


Fig. 7. Generated heat of the case A

Case B: The Pareto optimal solutions in this mode are shown in Table (4) for scenario S13. The maximum weakest membership function which is equal to 0.7416 is related to solution #16. Taking into account the min-max fuzzy satisfying method, solution #16 is selected as the best compromise solution. The cost of MG energy production is equal to \$3730.738. The emission is obtained as 55093.84 kg/day. In solution #1, which is focused on the minimization of the total cost of MG, the minimum value of MG is obtained as \$3702.019, whereas solution #20 aims to obtain the minimum emission which is equal to 53049.772 kg/day. Total operation cost of MG in solution #13 (case A) compared to solution #16 (case B) decreased about 15.2% in comparing with case A, although emission has decreased about 9.6%.

Figures (8), (9) illustrate the generated power and heat of Case B, respectively. As shown in Figure (8), PV, WT, fuel cell, CHP1, and CHP2 also power-only unit have participated in



Received: 06-06-2024

Revised: 15-07-2024

Accepted: 28-08-2024

power production in the scheduling for 24 hours. As output of the optimization program, the production capacity of solar cells and wind turbines is 0.67 MW and 0.34 MW, respectively. The production curve of solar cell and wind turbine is shown in this Figure for 24 hours. Considering the interconnection of MG and network, the MG has sold a part of power demand to the network. Moreover, CHP1 and CHP2 have contributed in power production continuously.

According to Figure (9), the heat production of CHP1 unit is more than those of other production units, because generating power and heat by it is cheaper than the other units.

Table 4. Pareto optimal solutions for short-term scheduling of micro-grid without DRP (Case-B) for scenario s13 as a highest probability

#	OF1 (\$/day)	OF2 (kg/day)	OF _{1,p.u.}	OF _{2,p.u.}	Min (OF _{1,p.u.} , OF _{2,p.u.})
1	3702.019	62492.116	1.0000	0.0000	0.0000
2	3703.3005	62250.364	0.9885	0.0256	0.0256
3	3703.8511	61738.806	0.9835	0.0798	0.0798
4	3704.1196	61227.997	0.9811	0.1339	0.1339
5	3704.5965	60716.822	0.9768	0.1880	0.1880
6	3705.0845	60205.162	0.9724	0.2422	0.2422
7	3705.2673	59693.895	0.9708	0.2963	0.2963
8	3706.0203	59182.443	0.9640	0.3505	0.3505
9	3706.4356	58671.466	0.9603	0.4046	0.4046
10	3707.6484	58159.877	0.9494	0.4588	0.4588
11	3709.3555	57649.056	0.9340	0.5129	0.5129
12	3711.2299	57138.207	0.9171	0.5670	0.5670
13	3713.2289	56627.485	0.8991	0.6211	0.6211
14	3717.1511	56116.492	0.8639	0.6752	0.6752
15	3723.3446	55605.35	0.8081	0.7293	0.7293
16	3730.738	55093.84	0.7416	0.7835	0.7416
17	3740.8601	54583.002	0.6505	0.8376	0.6505
18	3755.9061	54071.861	0.5152	0.8918	0.5152
19	3776.0458	53560.572	0.3340	0.9459	0.3340
20	3813.1642	53049.772	0.0000	1.0000	0.0000

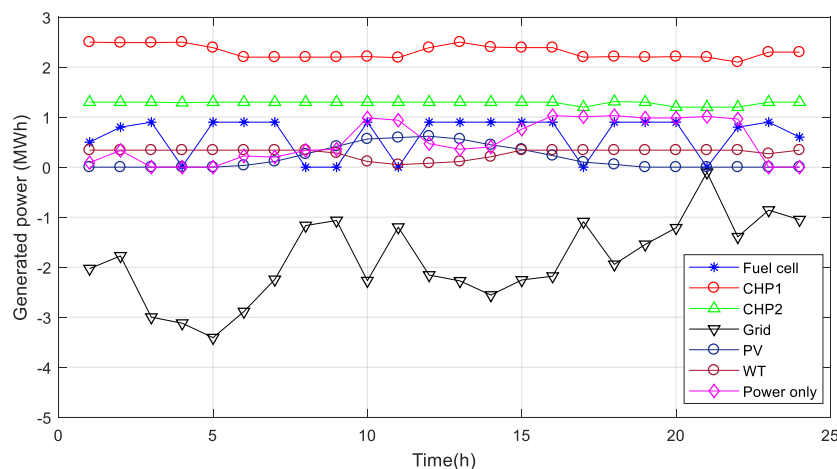


Fig. 8. Generated power of the case B.



Received: 06-06-2024

Revised: 15-07-2024

Accepted: 28-08-2024

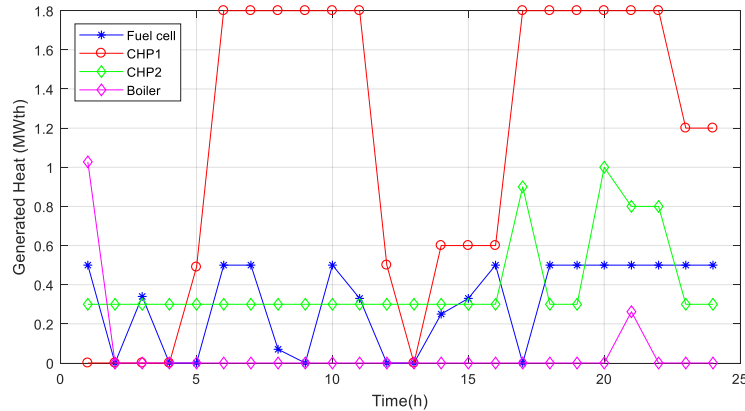


Fig. 9. Generated heat of the case B.

Case C: This case is analyzed for the determination of DRP's impact on the solution of MG scheduling. The Pareto optimal results for third case are presented in Table (5) and scenario S13. The maximum weakest membership function considering the prepared solutions in this table is equal to 0.7687, which is related to solution #16. According to the min-max fuzzy satisfying method, Solution#16 is the best compromise solution. The cost of MG energy production is equal to \$3609.356 and emission is obtained as 54341.95 kg/day. In solution #1, which is aimed to minimize cost, obtained value is \$3594.124. Also, the minimum value of operation emission is equal to 52712.029 kg/day, which is obtained in solution #20 where the emission minimization is aimed. By comparing with the second case, total cost in selected solution has decreased about 1.4% although emission has decreased about 3%. The results show the effectiveness of the TOU-DR program.

Table 5. Pareto optimal solutions for short-term scheduling of micro-grid considering DRP (Case-C) for scenario s13 as a highest probability

#	OF1 (\$/day)	OF2 (kg/day)	OF _{1,p.u.}	OF _{2,p.u.}	Min (OF _{1,p.u.} , OF _{2,p.u.})
1	3594.124	60189.17	1.0000	0.0000	0.0000
2	3594.1262	60047.954	1.0000	0.0189	0.0189
3	3594.59	59640.15	0.9929	0.0734	0.0734
4	3595.0403	59232.364	0.9861	0.1280	0.1280
5	3596.0522	58825.125	0.9707	0.1824	0.1824
6	3596.6727	58417.864	0.9613	0.2369	0.2369
7	3597.4428	58010.684	0.9496	0.2914	0.2914
8	3598.3417	57603.41	0.9360	0.3458	0.3458
9	3598.8486	57195.287	0.9283	0.4004	0.4004
10	3599.8584	56787.455	0.9129	0.4549	0.4549
11	3600.5629	56379.686	0.9022	0.5095	0.5095
12	3601.5667	55971.641	0.8870	0.5641	0.5641
13	3602.6033	55564.375	0.8713	0.6185	0.6185
14	3603.9396	55156.83	0.8510	0.6730	0.6730
15	3605.9495	54749.498	0.8205	0.7275	0.7275
16	3609.356	54341.95	0.7687	0.7820	0.7687
17	3615.4996	53934.708	0.6755	0.8365	0.6755
18	3621.9587	53527.247	0.5774	0.8910	0.5774
19	3634.8452	53120.039	0.3817	0.9454	0.3817
20	3659.9881	52712.029	0.0000	1.0000	0.0000



Received: 06-06-2024

Revised: 15-07-2024

Accepted: 28-08-2024

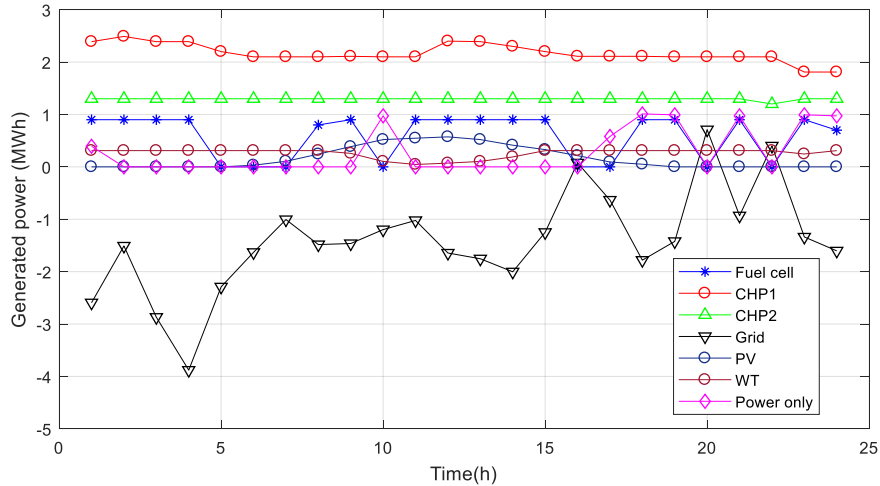


Fig. 10. Generated power of the case C.

Figure (10) illustrates the generated power and heat of case C. As shown in Figure (10), PV, WT, fuel cell, CHP1, and CHP2 also power-only unit have participated in power production in the scheduling for 24 hours. As output of the optimization program, the production capacity of solar cells and wind turbines is 0.62 MW and 0.31 MW, respectively. The production curve of solar cell and wind turbine is shown in this Figure for 24 hours. Considering the interconnection of MG and network, the MG has sold a part of power demand to the network also the MG has purchased a part of power demand from the network. Moreover, CHP1 and CHP2 have contributed in power production continuously.

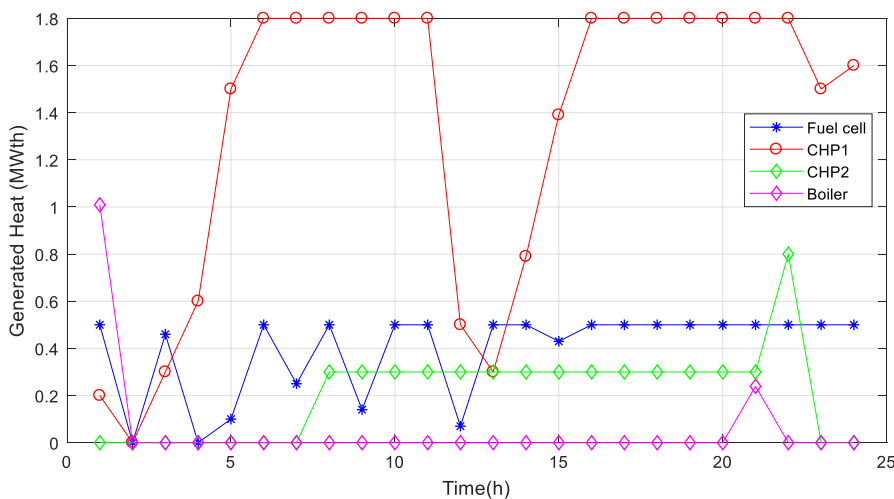


Fig. 11. Generated heat of the case C.

The heat generated of case C, for 24 hours is shown in Figure (11). The participation of CHP1 and fuel cell in the heat generation of MG is obvious, in which CHP1 has produced more heat than CHP2 due to its low cost function. Additionally, CHP2 and the boiler have less contribution to the heat generation of MG, since their cost functions are higher than those of



Received: 06-06-2024

Revised: 15-07-2024

Accepted: 28-08-2024

other generation units. It should be noted that the generated hydrogen has been stored in the hydrogen tank.

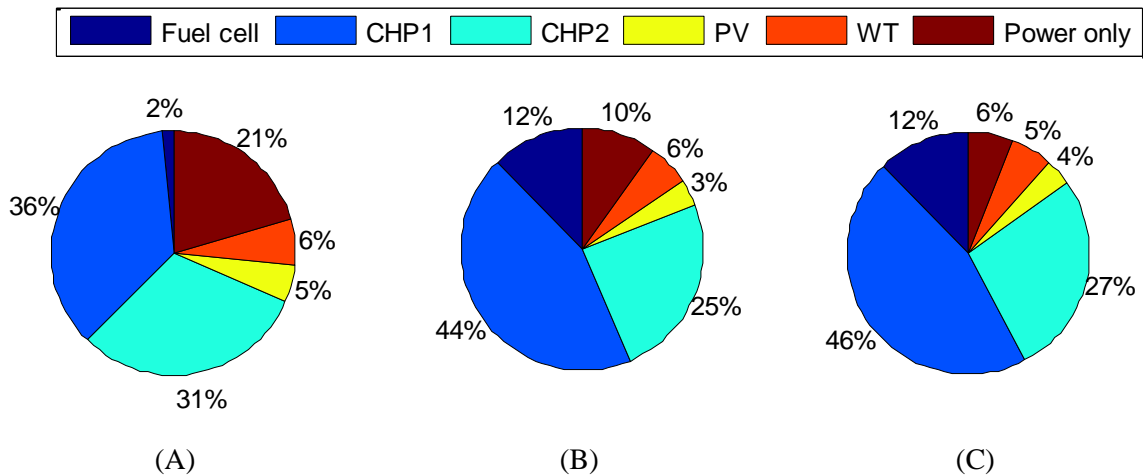


Fig. 13. Percentage of electric energy provided by the different components of the HMS for Cases A, B and C for scenario s13 as a highest probability

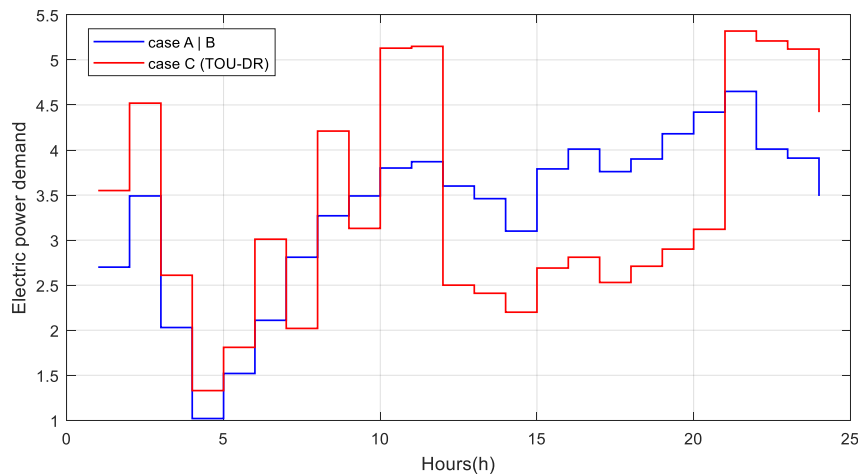


Fig. 14. Demand levels comparison with considering DRP

The contribution of the energy of each component (i.e. Fuel cell, CHP1, CHP2, PV panels, wind turbine and power only unit) for scenario s13 as a highest probability is given in Figure (13). The electric power demand with consideration of DRP implementation of case A or case B in comparison with case C is demonstrated in Figure (14). By applying DR program, load is shifted from high price period to inexpensive time periods. According to power prices shown in Figure (5), obviously, high price periods are experienced between $h = 12$ and $h = 16$. So, DR programs shift load from these periods to inexpensive periods which are between $h = 22$ and $h = 24$. It should be denoted that the amount of these changes in TOU-DR program is limited about 30%.

Optimal Pareto solutions using MOPSO algorithm as well as selected trade-off solution based on fuzzy satisfying approach are shown in Figure (15).



Received: 06-06-2024

Revised: 15-07-2024

Accepted: 28-08-2024

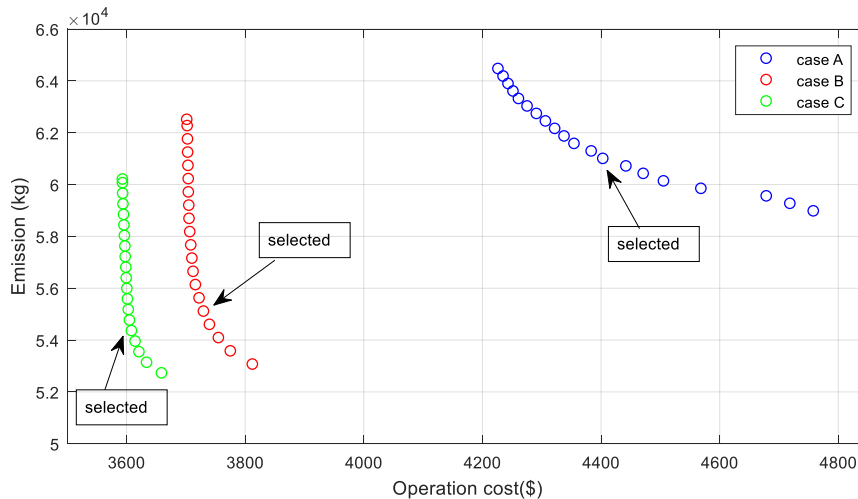


Fig. 15. Pareto solution front using MOPSO in three cases (A, B and C)

6. Conclusion

In this paper, scheduling of a MG is considered that the MG composed of FC unit, two types of CHP generating units, power only unit, PV, WT, boiler, ESS and heat storage. A demand response program (DRP) based on time-of-use is applied to power demands. The uncertainties related to load demand, wind speed and solar irradiation are modeled with a scenario-based stochastic modeling and expected values calculation are used to evaluate the effect of uncertainty in each case study. The proposed cost and emission functions are optimized simultaneously using MOPSO algorithm to solve the problem. Compromising between the Pareto front solutions is done using the fuzzy min-max satisfying method. In this study, three cases are analyzed to confirm the performance of the proposed approach, including islanded mode, grid connected mode, and the effect of the TOU-DR program on MG scheduling.

For the 27 scenarios, the multi-objective optimization problem was implemented in MATLAB environment and the best solution was selected from the Pareto solution front by fuzzy decision making. These selected solutions are shown in Table (6) for three cases (A, B and C) for each 27 scenarios. In Case A, MG is considered in the islanded mode; and the expected cost of energy production and expected emission cost are achieved 4499.8 \$/day and 61242.1 kg/day respectively. Also, in Case B, MG is in the grid-connected mode and the expected cost of energy production and expected emission cost are decreased to 3763.6 \$/day and 57158.4 kg/day, respectively. Finally by implementing the DR program in Case C, the expected cost of energy production and expected emission cost are 3632.7 \$/day and 56014.4 kg/day, respectively.

It can be concluded that connecting the MG to the power grid reduces the cost of operation and the cost of pollution compared to the isolated mode. Also, using demand response programs helps to further improve these objective functions.



Received: 06-06-2024

Revised: 15-07-2024

Accepted: 28-08-2024

Table 6. The total cost (\$/day) and total Emission (kg/day) for case A, B and C under each scenario and related expected values

Scenario	π_S	Case A		Case B		Case C	
		OF1 (\$/day)	OF2 (kg/day)	OF1 (\$/day)	OF2 (kg/day)	OF1 (\$/day)	OF2 (kg/day)
S1	0.0201	4635.506	61480.76	3829.395	60285.39	3637.147	54570.19
S2	0.0043	4710.852	59914.99	3730.01	53330.21	3642.378	55394.72
S3	0.001	4619.357	62104.85	3847.255	53201.03	3675.171	59150.57
S4	0.0553	4524.526	63429.93	3792.544	57920.99	3685.603	55955.46
S5	0.0119	4461.651	58907.67	3834.579	61001.77	3673.366	59169.5
S6	0.0028	4521.26	58968.44	3757.389	59899.39	3568.785	57184.45
S7	0.0499	4460.692	59991.95	3720.421	54764.15	3658.964	57570.94
S8	0.0107	4576.45	62518.11	3790.889	55805.05	3645.622	56950.12
S9	0.0026	4486.267	60536.11	3846.614	59299.05	3591.379	56968.01
S10	0.0866	4694.652	61300.43	3722.138	56346.28	3646.696	53729.82
S11	0.0186	4563.607	58596.48	3724.21	53961.43	3576.273	60442.26
S12	0.0044	4290.116	61651.08	3711.271	61795.89	3655.666	53736.21
S13	0.238	4403.956	60984.88	3730.738	55093.84	3609.356	54341.95
S14	0.051	4473.845	60348.21	3732.119	57615.13	3633.332	57784.36
S15	0.0122	4450.063	62743.93	3724.888	55169.17	3626.649	56299.75
S16	0.2149	4480.744	61693.01	3826.323	60568.99	3641.805	58696.22
S17	0.0461	4731.023	60947.91	3791.431	57785.82	3635.298	58077.5
S18	0.011	4527.646	62174.24	3735.91	55887.64	3659.393	53444.2
S19	0.0201	4555.719	61944.11	3716.551	58012.13	3630.778	56184.1
S20	0.0043	4393.816	63136.5	3843.625	61129.92	3670.03	55194.38
S21	0.001	4374.869	64360.62	3803.741	56364.97	3595.626	59047.06
S22	0.0553	4426.011	61566.56	3764.478	56187.7	3636.445	52809.49
S23	0.0119	4790.716	63652.67	3761.438	62354.22	3584.729	59213.3
S24	0.0028	4756.234	58725.11	3730.415	53100.11	3587.354	54702.96
S25	0.0499	4443.578	60375.65	3730.942	54123.01	3604.453	53393.77
S26	0.0107	4476.029	59274.14	3791.297	53802.65	3637.283	52758.33
S27	0.0026	4328.805	61377.62	3742.025	57692.54	3641.118	53322.01
Expected value		4499.8	61242.1	3763.6	57158.4	3632.7	56014.4

7. References

- [1] Y. Zhang, F. Meng, R. Wang, B. Kazemtabrizi, J. Shi, "Uncertainty-resistant stochastic MPC approach for optimal operation of CHP microgrid", *Energy*, Volume 179, 15 July 2019, Pages 1265-1278
- [2] A.R. Nouri, H. Khodaei, A. Darvishan, S. M. Sharifian, N. Ghadimi, "Optimal performance of fuel cell-CHP-battery based micro-grid under real-time energy management: An epsilon constraint method and fuzzy satisfying approach" *Energy* Volume 159 April 2018 Page 121-133
- [3] H. Pashaei-Didani, S. Nojavan, R. Nourollahi, K. Zare, "Optimal economic-emission performance of fuel cell/CHP/storage based microgrid," *International Journal of Hydrogen Energy* Vol. 44, Issue 138 March 2019 Pages 6896-6908.
- [4] Hongxia YU, Kun ZHANG, Yuying LIU, Junwen DAI, Zhenting SUN, "Micro-grid Scheduling of Electric Boiler and CHP with Thermal Energy Storage Based on Wind Power Accommodating," 2019 IEEE 10th International Symposium on Power Electronics and Distributed Generation Systems (PEDG)
- [5] V. Tiwari, H. Mohan Dubey, M. Pandit and S. Reddy Salkuti, "CHP-Based Economic Emission Dispatch of Microgrid Using Harris Hawks Optimization," *Fluids* 2022, 7, 248. <https://doi.org/10.3390/fluids7070248>
- [6] M. Motevasel and A. R. Seifi, "Expert energy management of a microgrid considering wind energy uncertainty," *Energy Convers. Manage.*, vol. 83, pp. 58–72, 2014.



Received: 06-06-2024

Revised: 15-07-2024

Accepted: 28-08-2024

- [7] X. Song, R. Zhao, G. De, J. Wu, H. Shen, Z. Tan, J. Liu, "A fuzzy-based multi-objective robust optimization model for a regional hybrid energy system considering uncertainty," *Energy Sci Eng.* 2020; 1–18.
- [8] S. Mohammadi, S. Soleymani, and B. Mozafari, "Scenario-based stochastic operation management of microgrid including wind, photovoltaic, micro-turbine, fuel cell and energy storage devices," *Int. J. Elect. Power Energy Syst.*, vol. 54, pp. 525–535, 2014.
- [9] A. Najafi, M. Marzband, B. Mohamadi-Ivatloo, J. Contreras, M. Pourakbari-Kasmaei, M. Lehtonen and R. Godina, "Uncertainty-Based Models for Optimal Management of Energy Hubs Considering Demand Response," *Energies* 2019, 12, 1413; doi:10.3390/en12081413.
- [10] H. Rafik El-Hana Bouchekara, M. Sharjeel Javaid, Y. Abubakar Shaaban, M. Shoaib Shahriar, M. Anwari Muhammad Ramli, Y. Latreche, "Decomposition based multiobjective evolutionary algorithm for PV/Wind/Diesel Hybrid Microgrid System design considering load uncertainty," *Energy Reports* 7 (2021) 52–69
- [11] K. H. Nunna and S. Doolla, "Responsive end-user-based demand side management in multi microgrid environment," *IEEE Trans. Ind. Informat.*, vol. 10, no. 2, pp. 1262–1272, May 2014.
- [12] R. Deng, R. Lu, G. Xiao, and J. Chen, "Fast distributed demand response with spatially-and temporally-coupled constraints in smart grid," *IEEE Trans. Ind. Informat.*, Mar. 2015, doi: 10.1109/TSG.2013.2290971.
- [13] A. Rabiee, A. Soroudi, B. Mohammadi-ivatloo, and M. Parniani, "Corrective voltage control scheme considering demand response and stochastic wind power," *IEEE Trans. Power Syst.*, vol. 29, no. 6, pp. 2965–2973, Nov. 2014.
- [14] Y. Ding, S. Hong, and X. Li, "A demand response energy management scheme for industrial facilities in smart grid," *IEEE Trans. Ind. Informat.*, vol. 10, no. 4, pp. 2257–2269, Nov. 2014.
- [15] A. Safdarian, M. Fotuhi-Firuzabad, and M. Lehtonen, "A distributed algorithm for managing residential demand response in smart grids," *IEEE Trans. Ind. Informat.*, vol. 10, no. 4, pp. 2385–2393, Nov. 2014.
- [16] D.-M. Kim and J.-O. Kim, "Design of emergency demand response program using analytic hierarchy process," *IEEE Trans. Smart Grid*, vol. 3, no. 2, pp. 635–644, Jun. 2012.
- [17] Ahmad Alzahrani, Muhammad Arsalan Hayat, Asif Khan, Ghulam Hafeez, Farrukh Aslam Khan, Muhammad Iftikhar Khan, Sajjad Ali, "Optimum sizing of stand-alone microgrids: Wind turbine, solar photovoltaic, and energy storage system," *Journal of Energy Storage* 73 (2023) 108611.
- [18] M. Kazemi, B. Mohammadi-Ivatloo, and M. Ehsan, "Risk-based bidding of large electric utilities using information gap decision theory considering demand response," *Elect. Power Syst. Res.*, vol. 114, pp. 86–92, 2014.
- [19] Z. Zhu, S. Lambbotharan, W. Chin, and Z. Fan, "A game theoretic optimization framework for home demand management incorporating local energy resources," *IEEE Trans. Ind. Informat.*, vol. 11, no. 2, pp. 353–362, Apr. 2015.
- [20] A. H. Eshraghi, G. R. Salehi, S. M. Heibati, K. Lari, "An assessment of the effect of different energy storage technologies on solar power generators for different power sale scenarios: The case of Iran," *Sustainable Energy Technologies and Assessments Volume 34*, August 2019, Pages 62-67
- [21] J. Aghaei and M.-I. Alizadeh, "Multi-objective self-scheduling of CHP (combined heat and power)-based microgrids considering demand response programs and ESS (energy storage systems)," *Energy*, vol. 55, pp. 1044–1054, 2013.
- [22] Ho-Sung Ryu and Mun-Kyeom Kim, "Two-Stage Optimal Microgrid Operation with a Risk-Based Hybrid Demand Response Program Considering Uncertainty," *Energies* 2020, 13, 6052; doi:10.3390/en13226052.
- [23] A. J. Conejo, M. Carrion, and J. M. Morales, *Decision Making Under Uncertainty in Electricity Markets*, vol. 153. New York, NY, USA: Springer, 2010.
- [24] A. H. Eshraghi, G. R. Salehi, S. M. Heibati, K. Lari, "An enhanced operation model for energy storage system of a typical combined cool, heat and power based on demand response program: The application of mixed integer linear programming," *Building Serv. Eng. Res. Technol.* 2019, Vol. 40(1) 47–74
- [25] A. H. Eshraghi, G. R. Salehi, S. M. Heibati, K. Lari, "Developing operation of combined cooling, heat, and power system based on energy hub in a micro-energy grid: The application of energy storages," *Energy & Environment*, 2019, 0(0) 1-24, doi:10.1177/0958305x19846577
- [26] T. Niknam, R. Azizipanah-Abarghooee, M. Rasoul Narimani, "An efficient scenario-based stochastic programming framework for multi-objective optimal micro-grid operation," *Applied Energy* 99 (2012) 455–470
- [27] A. Ramadan, M. Ebeed, S. Kamel, A. Y. Abdelaziz and H. Haes Alhelou, "Scenario-Based Stochastic Framework for Optimal Planning of Distribution Systems Including Renewable-Based DG Units," *Sustainability* 2021, 13, 3566. <https://doi.org/10.3390/su13063566>



Received: 06-06-2024

Revised: 15-07-2024

Accepted: 28-08-2024

- [28] L. He, Z. Lu, L. Pan, H. Zhao, X Li and J Zhang, "Optimal Economic and Emission Dispatch of a Microgrid with a Combined Heat and Power System," *Energies* 2019, 12, 604; doi:10.3390/en12040604
- [29] Majidi M, Nojavan S, Zare K. "Optimal stochastic short-term thermal and electrical operation of fuel cell/ photovoltaic/ battery/ grid hybrid energy system in the presence of demand response program," *Energy Conversion and Management* 2017 Jul 15; 144:132-42.
- [30] M Taghizadeh, S Bahramara, F Adabi, S Nojavan, "Optimal operation of storage-based hybrid energy system considering market price uncertainty and peak demand management," *Journal of Energy Storage* 30 (2020) 101519
- [31] Nazari-Heris M, Abapour S, Mohammadi-Ivatloo B. "Optimal economic dispatch of FC-CHP based heat and power micro-grids," *Applied Thermal Engineering* 2017 Mar 5; 114: 756-69.
- [32] G.R. Aghajani, H.A. Shayanfar, H. Shayeghi, "Presenting a multi-objective generation scheduling model for pricing demand response rate in micro-grid energy management," *Energy Conversion and Management* 106 (2015) 308–321
- [33] Coello Coello CA, Lechuga MS, editors. "MOPSO: a proposal for multiple objective particle swarm optimization," In: *IEEE 2002 CEC'02 proceedings of the 2002 congress on evolutionary computation*; 2002.